



## 저작자표시-비영리-변경금지 2.0 대한민국

이용자는 아래의 조건을 따르는 경우에 한하여 자유롭게

- 이 저작물을 복제, 배포, 전송, 전시, 공연 및 방송할 수 있습니다.

다음과 같은 조건을 따라야 합니다:



저작자표시. 귀하는 원저작자를 표시하여야 합니다.



비영리. 귀하는 이 저작물을 영리 목적으로 이용할 수 없습니다.



변경금지. 귀하는 이 저작물을 개작, 변형 또는 가공할 수 없습니다.

- 귀하는, 이 저작물의 재이용이나 배포의 경우, 이 저작물에 적용된 이용허락조건을 명확하게 나타내어야 합니다.
- 저작권자로부터 별도의 허가를 받으면 이러한 조건들은 적용되지 않습니다.

저작권법에 따른 이용자의 권리는 위의 내용에 의하여 영향을 받지 않습니다.

이것은 [이용허락규약\(Legal Code\)](#)을 이해하기 쉽게 요약한 것입니다.

[Disclaimer](#)

Master's Thesis

Nitrate-based aprotic electrolyte for reversible Li-CO<sub>2</sub> battery

Seongho Woo

Department of Energy Engineering  
(Battery Science and Technology)

Graduate School of UNIST

2020

# Nitrate-based aprotic electrolyte for reversible Li- CO<sub>2</sub> battery

Seongho Woo

Department of Energy Engineering  
(Battery Science and Technology)

Graduate School of UNIST


# Nitrate-based aprotic electrolyte for reversible Li- CO<sub>2</sub> battery

A thesis/dissertation  
submitted to the Graduate School of UNIST  
in partial fulfillment of the  
requirements for the degree of  
Master of Science

Seongho Woo

12/03/2019 of submission

Approved by



Advisor

Seok Ju Kang

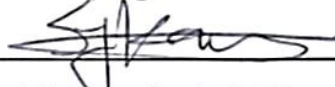
Nitrate-based aprotic electrolyte for reversible Li-CO<sub>2</sub> battery

Seongho Woo

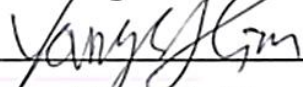
This certifies that the thesis/dissertation of Seongho Woo is approved.

12/03/2019


signature

  
\_\_\_\_\_  
Advisor: Seok Ju Kang

signature

  
\_\_\_\_\_  
Youngsik Kim

signature

  
\_\_\_\_\_  
Nam-Soon Choi

## Contents

Abstract.....	6
List of figures.....	7
Chapter 1 Reversible reaction of Li-CO <sub>2</sub> battery.....	8
1.1 Introduction of Li-CO <sub>2</sub> battery.....	8
1.2 Trends of Li-CO <sub>2</sub> research.....	10
1.2.1 Electrodes	
1.2.2 Kinds of catalysts	
1.2.3 Redox mediators (RMs)	
1.3 Goal for in this research.....	14
1.4 Result and discussion.....	15
1.4.1 Consumption of CO <sub>2</sub> during discharge	
1.4.2 Discharge product analysis in nitrate-based electrolyte	
1.4.3 Evolution of CO <sub>2</sub> using DEMS analysis	
1.4.4 High concentration effect of nitrate-based electrolyte	
1.5 Conclusion.....	21
1.6 Experimental section.....	22
References.....	23

## Abstract

Recently, the Li-CO<sub>2</sub> batteries have emerged as fascinating energy storage system because of capturing CO<sub>2</sub> and converting into valuable energy. However, the Li<sub>2</sub>CO<sub>3</sub> as the discharge product has insulating property in Li-CO<sub>2</sub> batteries where exhibits more sluggish decomposition reaction kinetics, and it leads to the increase of the overpotential during charging. In this study, we demonstrate reversible operation of the Li-CO<sub>2</sub> battery with LiNO<sub>3</sub>-based aprotic electrolyte. Our quantitative study on in-situ differential electrochemical mass spectrometry (DEMS) investigation with LiNO<sub>3</sub>-based electrolyte in Li-CO<sub>2</sub> battery reveals the equal consumption/evolution of CO<sub>2</sub> gases during discharge/charge process. Li-CO<sub>2</sub> battery using LiNO<sub>3</sub>-based electrolyte shows the two-electron reversible reaction. In particular, the NO<sub>3</sub><sup>-</sup> ions acts redox mediator during discharge/charge process where efficiently changes the reaction route from irreversible 1.33 e<sup>-</sup>/CO<sub>2</sub> to reversible 2.00 e<sup>-</sup>/CO<sub>2</sub>. And we demonstrate the discharge product, which is the Li<sub>2</sub>CO<sub>3</sub>, according to X-ray photoelectron spectroscopy (XPS) and Raman spectroscopy (Raman) results. This study indicates that the LiNO<sub>3</sub>-based electrolyte offer highly reversible Li-CO<sub>2</sub> operation with redox-shuttle effect.

## List of figures

**Figure 1.1** The schematic illustration of Li-O<sub>2</sub> and CO<sub>2</sub> battery's structure/mechanism.

**Figure 1.2** The schematic illustration of side-reaction during decomposition of Li<sub>2</sub>CO<sub>3</sub>

**Figure 1.3** The schematic illustrations of electrode components.

**Figure 1.4** The schematic illustrations of catalyst's challenge.

**Figure 1.5** The schematic of principle & function of redox mediator.

**Figure 1.6** The quantities of CO<sub>2</sub> gas consumption occur during discharge. a) uses the LiTFSI in TEGDME electrolyte. b) uses the LiNO<sub>3</sub> in the DMAc electrolyte. The blue line in both graphs indicates the potential. Black and green lines indicate CO<sub>2</sub> gas consumption during discharge. (The orange dotted line is the gas consumption according to 1.33 electron process. The red dotted line is the gas consumption according to 2.00 electron process.).

**Figure 1.7** Discharge product analysis in LiNO<sub>3</sub>-based electrolyte using a) and b) XPS, c) Raman and SEM, applying a current of 200  $\mu$ A for 5 hours. a), b) are the XPS data of pristine cathode and after discharge respectively. c) is the Raman data. (the black line is the pristine cathode, the red line is the after discharge, while the orange symbol (#) is the Raman peak of Li<sub>2</sub>CO<sub>3</sub>  $\sim$  1088 cm<sup>-1</sup>).

**Figure 1.8** The first charge and CO<sub>2</sub> gas evolution profiles of Li-CO<sub>2</sub> cell, applying a current of 200  $\mu$ A for 5 hours obtained using DEMS analysis in a) the LiTFSI-based electrolyte and b) the LiNO<sub>3</sub>-based electrolyte after 1.0 mAh discharged at pure CO<sub>2</sub> atmosphere.

**Figure 1.9** The first discharge a) and charge b) profiles with high concentration 3 M LiNO<sub>3</sub> in DMAc electrolyte. CO<sub>2</sub> gas reduction and oxidation profiles during discharge and charge process of Li-CO<sub>2</sub> cell, applying a current of 200  $\mu$ A for 5 hours obtained using in-situ DEMS analysis.

**Figure 1.10** Schematic illustration of the suggestion mechanism in Li-CO<sub>2</sub> using LiNO<sub>3</sub>-based electrolyte.



## Chapter 1

### 1.1 Introduction of Li-CO<sub>2</sub> battery

Over time, the negative effect of carbon dioxide (CO<sub>2</sub>) gases, the most dominant greenhouse gas, on the atmospheric warming has been increasing because of the excessive use of fossil fuels.<sup>1</sup> To convert CO<sub>2</sub> gas into other organic compounds, a significant energy input is needed because carbon atom has the highest oxidation state.<sup>2</sup> In order to fix CO<sub>2</sub>, various products are obtained, including methanol,<sup>3</sup> ethylene<sup>4</sup> and carbon monoxide.<sup>5</sup> Nevertheless, these chemicals require further compression process treatment to store and transport conveniently. This process gives rise to additional energy consumption. Accordingly, fixing CO<sub>2</sub> could suggest an alternative by using renewable energy in an energy storage device.

Intriguingly, a study on Li-CO<sub>2</sub> battery has been emerged in recent years.<sup>6</sup> Because Li-CO<sub>2</sub> batteries can capture CO<sub>2</sub> gas, which has been used to store the energy as an energy carrier. Generally, Li-CO<sub>2</sub> batteries compose of a Li metal anode, an electrolyte, a separator and a carbon-based cathode. The electrochemical reaction in Li-CO<sub>2</sub> batteries are expressed as  $4\text{Li} + 3\text{CO}_2 \leftrightarrow 2\text{Li}_2\text{CO}_3 + \text{C}$  ( $E^\circ = 2.8 \text{ V}$ , Figure 1.1), where Li<sub>2</sub>CO<sub>3</sub> and C (carbon) are the main discharge products in

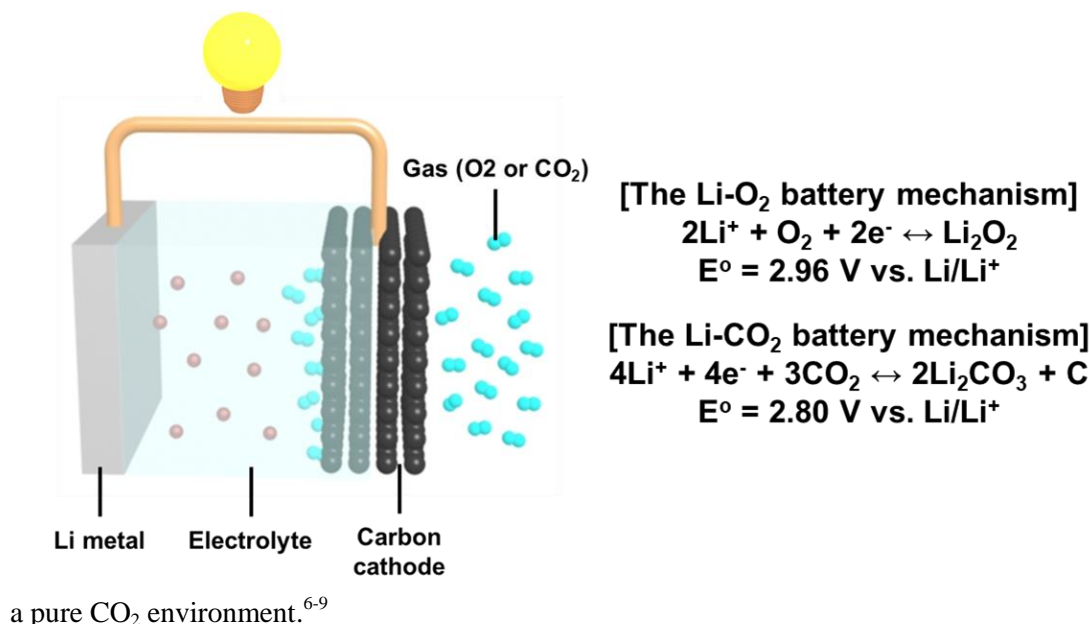


**Figure 1.1** The schematic illustration of Li-O<sub>2</sub> and CO<sub>2</sub> battery's structure/mechanism

However, the decomposition of  $\text{Li}_2\text{CO}_3$  requires high energy owing to its insulating properties and results in an increased overpotential. The high overpotential causes the further decomposition of the electrolyte, leading to the reducing of the amount of electrolyte in the battery and then the side reaction and poor cycling stability of the battery. These significant problems negate the advantages of Li- $\text{CO}_2$  batteries.<sup>10</sup>

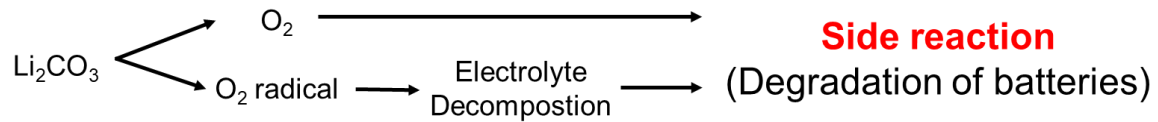


**Figure 1.2** The schematic illustration of side-reaction during decomposition of  $\text{Li}_2\text{CO}_3$

To improve Li- $\text{CO}_2$  battery performance, the discharge product must be efficiently decomposed, and the decomposition reactions of the electrolyte must be suppressed. Recently, many studies have been focusing on the improvement of electrode design, catalyst, and electrolyte to address the challenges on Li- $\text{CO}_2$  batteries.

## 1.2 Trends of Li-CO<sub>2</sub> battery studies

### 1.2.1 Electrodes

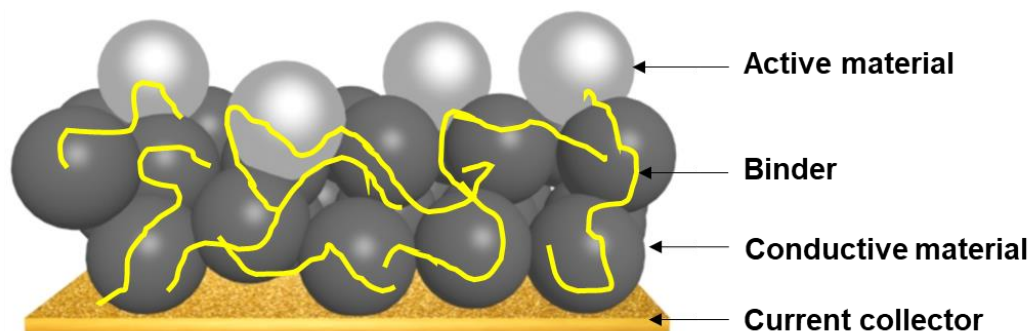


**Figure 1.3**  
 The schematic

illustration of electrode components.

Electrodes consist of an active material, a binder, a conductive material, and a current collector. (Figure 1.2) The conductive material, usually using carbon materials, transports the electrons which are generated after the electrochemical reaction, from the active materials to the current collector. The electric flow interference, resulting from the decomposition of the electrolyte and the electrode, causes the overpotential and the cell performance degradation.<sup>11</sup> Therefore, studies have been conducted on using high conductivity electrodes that prevent the decomposition of the electrode.

Dai's groups have recently proposed the anodes in which graphene, a high specific surface area and conductivity material, is doped with heteroatoms (B, N).<sup>12</sup>

Subsequently, the carbon nanotubes (CNT), owing to its high porosity and conductivity, has been reported to obtain higher cycle performance of the battery than graphene. These cathodes have long-term cycle stability than only carbon-based cathodes.<sup>13-14</sup>

However, the problem of those approaches is that traces of Li<sub>2</sub>CO<sub>3</sub> still remains after long-term cycling. In addition, the cycle and capacity do not reach the level of Li-CO<sub>2</sub> battery use. Therefore, Li-CO<sub>2</sub> battery has been studied various cathodes and catalysts to reduce overpotential and to improve cycle performance through reversible reactions.

### 1.2.2 Kinds of catalysts

Carbon-based cathodes require a lot of energy for  $\text{Li}_2\text{CO}_3$  insulator decomposition. Also, there is the concern that the unnecessary energy released would cause overpotential resulting in the decomposition of the electrode and the electrolyte. To achieve reversible  $\text{Li}_2\text{CO}_3$  decomposition, studies are being conducted on using carbon-based cathode with catalysts.

Catalysts are synthesized by novel metals or transition metals and used to enhance the decomposition of the  $\text{Li}_2\text{CO}_3$  discharge product. Studies have been performed using catalysts in  $\text{Li-CO}_2$  batteries. Catalysts on electrodes have been used to improve battery performance and efficiency through higher capacity and lower overpotential than carbon-based cathodes.<sup>15-21</sup>

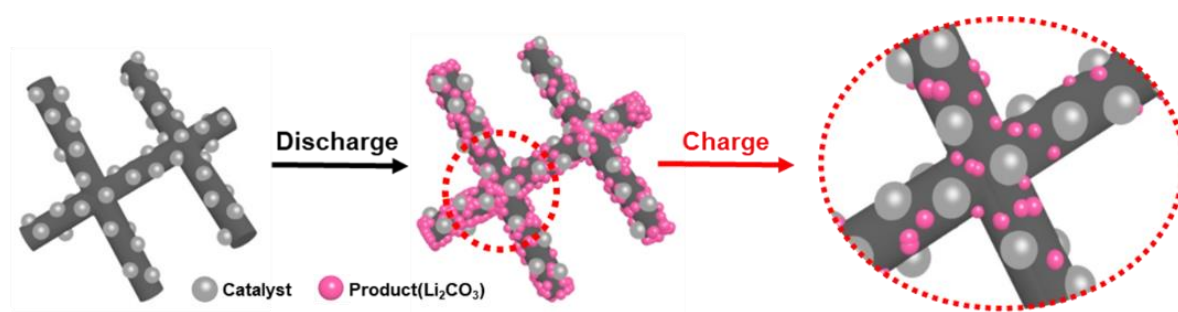


**Figure 1.4** The schematic illustration of catalyst's challenge.[21]

Nevertheless, there is a problem in which small amounts of  $\text{Li}_2\text{CO}_3$  still remain after long-term cycling. In this phenomenon, the areas of adjacent to the catalyst can easily decompose  $\text{Li}_2\text{CO}_3$  discharge product, but the areas that are far from the catalyst cannot decompose easily (Figure 1.4). Studies are being conducted to increase the catalytic reactivity of catalysts that are highly dispersible, and more progress is needed. Furthermore, most catalysts are expensive owing to their scarcity, and only the adjacent areas of existing dispersed catalyst electrodes are decomposed.<sup>19-21</sup>

To compensate for these shortcomings, this study elucidates a redox mediator, which is dissolved in a solvent, lowers overpotential, and increases reactivity with the product.

### 1.2.3 Redox mediators (RMs)

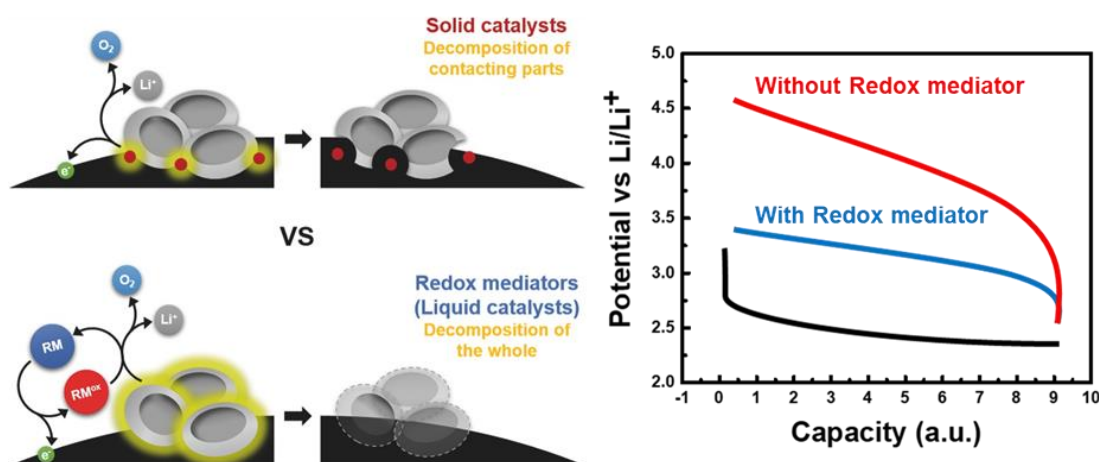


**Figure 1.5** The schematic of principle & function of redox mediator.[22]

RM stands for “redox mediator”, and directly participates in the redox reaction. RM not only reduces the de-composition-activation energy of the discharge products but also acts as a catalyst during the charge process. As a catalyst dissolves in an organic solvent, it increases contact areas with the discharge product and selectively decomposes only the product. In addition, an RM has the advantage of allowing the battery to operate via a reversible reaction through directly engaging in the electrochemical reaction (Figure 1.5).<sup>22</sup>

Of the various types of RMs, studies have been reported on the active use of halogen and/or aromatic materials, which are stabilized after accepting or contributing electrons. The use of those RMs assist the stable redox reaction occurring within a low voltage range during the cycling of the batteries.<sup>23</sup>

To overcome these problems of Li-CO<sub>2</sub> battery studies, LiBr<sup>24</sup> and binuclear cobaltphthalocyanine<sup>25</sup> have been used. It reduced the overpotential than conventional organic solvent electrolytes, and Li<sub>2</sub>CO<sub>3</sub> was completely decomposed.

However, RMs react with lithium metal electrodes, and side reactions occur, due to their vulnerability of Li metal and reductive RMs.<sup>26</sup> These challenges must be improved in order for Li-CO<sub>2</sub> batteries to run.

Currently, studies on Li-CO<sub>2</sub> batteries are actively being conducted. Because there is scarce study data on Li-CO<sub>2</sub> battery, most of the Li-CO<sub>2</sub> battery studies have been conducted by referring to previous Li-O<sub>2</sub> battery studies.

In order to improve the decomposition of  $\text{Li}_2\text{CO}_3$  as the main discharge product and operate reversible reactions without side-reactions; there is on-going research on electrodes, catalysts, RMs and various electrolytes to overcome the problem of Li- $\text{CO}_2$  batteries.

### 1.3 Goal for in this research

This study used the  $\text{LiNO}_3$ -based aprotic electrolyte, in which  $\text{LiNO}_3$  salt used in  $\text{Li-O}_2$  battery, to increase the stability of the electrodes and improve the cycle performance of the battery.

Among the various studies to improvement performance that have been operated to reduce overpotential and pre-vent side-reactions in  $\text{Li-O}_2$  batteries, there have used  $\text{LiNO}_3$  salt with dimethylacetamide (DMAc) solvent.

$\text{Li}_2\text{O}$  forms on the electrode through the interaction between lithium metal anode and  $\text{NO}_3^-$  anion, and is a chemically stable solid electrolyte interphase (SEI) layer. The SEI layer prevents additional reactions from occurring on the electrode surface and produces ideal oxygen evolution reaction.<sup>27-29</sup> In the case of  $\text{LiNO}_3$ -based electrolytes, previous studies have operated batteries without the side-reactions caused by the  $\text{LiNO}_3$  salt's redox effect.<sup>30-31</sup> DMAc solvents have a high donor number, and they can stabilize radical species.<sup>32</sup>

This study shows the advantages of  $\text{LiNO}_3$  and DMAc solvent in  $\text{Li-CO}_2$  batteries in order to resolve the irreversible reactions problem associated with  $\text{Li-CO}_2$  batteries. XPS, SEM (scanning electron microscope), and Raman were used to analyze the discharge products and to measure  $\text{CO}_2$  consumption with the DEMS analysis<sup>33</sup> method.

#### 1.4 Result and discussion

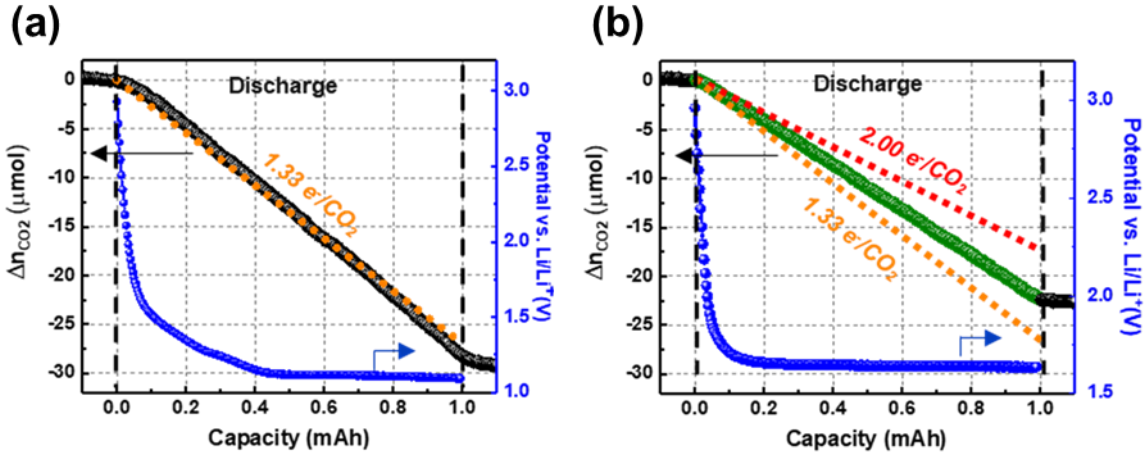


**Figure 1.6** The quantities of CO<sub>2</sub> gas consumption occur during discharge. a) uses the LiTFSI in TEGDME electrolyte. b) uses the LiNO<sub>3</sub> in the DMAC electrolyte. The blue line in both graphs indicates the potential. Black and green lines indicate CO<sub>2</sub> gas consumption during discharge. (The orange dotted line is the gas consumption according to 1.33 electron process. The red dotted line is the gas consumption according to 2.00 electron process.)

Figure. 1.6 a) is a graph that depicts the LiTFSI-based Li-CO<sub>2</sub> battery operating at a constant current of 200 μA. The graph shows the voltage and the amount of CO<sub>2</sub> consumed during discharge using the DEMS method. Figure 1.6 b) shows the measurements of the amount of CO<sub>2</sub> gas that is consumed when a LiNO<sub>3</sub>-type Li-CO<sub>2</sub> battery is discharged at a constant current of 200 μA.

Previous Li-CO<sub>2</sub> battery studies have shown a ( $4\text{Li} + 3\text{CO}_2 \leftrightarrow 2\text{Li}_2\text{CO}_3 + \text{C}$ ) mechanism of 1.33 e<sup>-</sup>/CO<sub>2</sub>, but the LiNO<sub>3</sub> type electrolyte shows around 1.7 e<sup>-</sup>/CO<sub>2</sub>. This electron process shows a different trend than previous studies. Therefore, several analysis techniques were used to confirm that the Li-CO<sub>2</sub> battery's main product Li<sub>2</sub>CO<sub>3</sub> was produced without additional reactions during discharge.



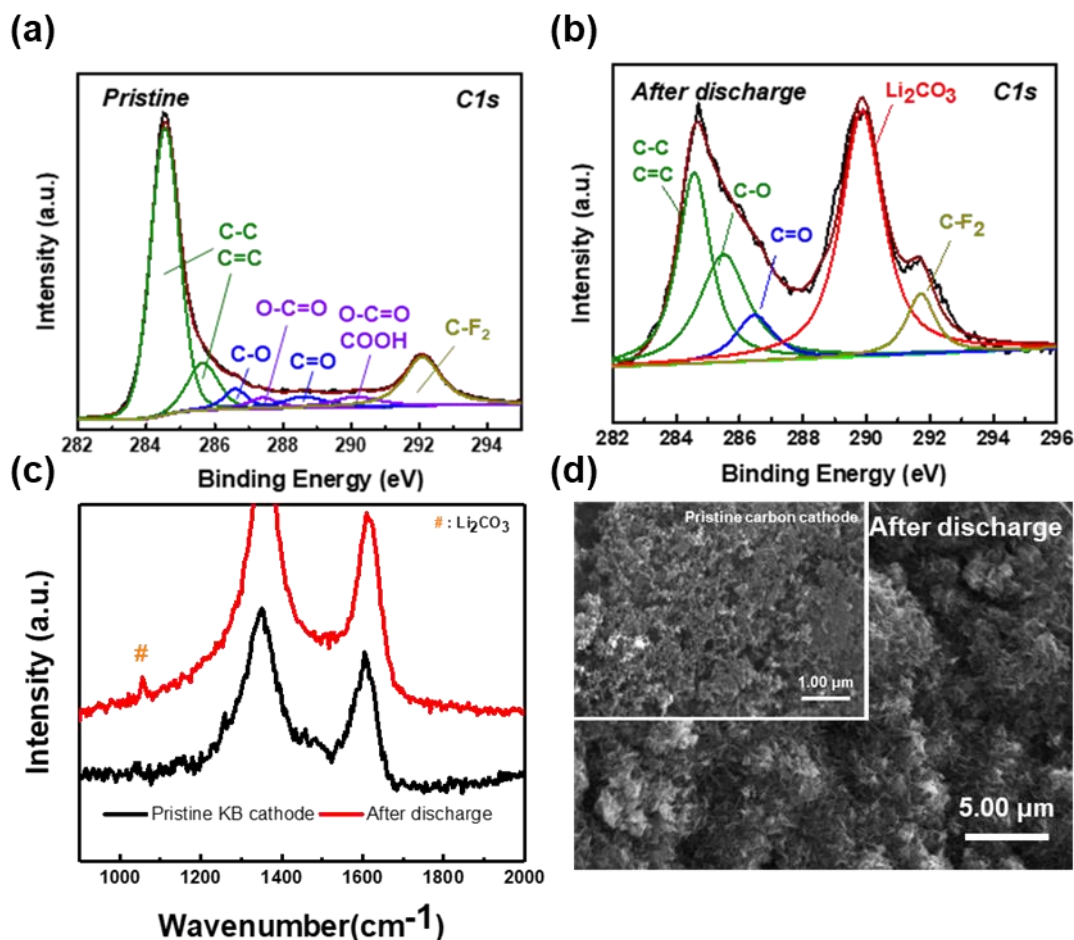


**Figure 1.7** Discharge product analysis in  $\text{LiNO}_3$ -based electrolyte using a) and b) XPS, c) Raman and SEM, applying a current of  $200 \mu\text{A}$  for 5 hours. a), b) are the XPS data of pristine cathode and after discharge respectively. c) is the Raman data. (the black line is the pristine cathode, the red line is the after discharge, while the orange symbol (#) is the Raman peak of  $\text{Li}_2\text{CO}_3$   $\sim 1088 \text{ cm}^{-1}$ )

Figure 1.7 is XPS, Raman, and SEM analysis to show the discharge product of the  $\text{LiNO}_3$  type  $\text{Li-CO}_2$  battery. Figure 1.7 a) shows the XPS analysis technique to measure the electrode before discharge, and Figure 1.7 b) shows the XPS results for the electrode surface specimen after discharge. When compared with Fig. 1.7 a), a peak ( $\sim 290 \text{ eV}$ ) for  $\text{Li}_2\text{CO}_3$  can be seen in Fig. 1.7 b). Fig. 1.7 C) shows a  $\text{Li}_2\text{CO}_3$  peak ( $\sim 1080 \text{ cm}^{-1}$ ) after discharge using the Raman analysis method.<sup>6,17,21,34-35</sup> Additional products were not seen in either the XPS or the Raman results. This can be interpreted to mean that the  $\text{LiNO}_3$ -type  $\text{Li-CO}_2$  battery mainly produces  $\text{Li}_2\text{CO}_3$ . Fig.1.7 d shows the SEM analysis technique. After discharge, the product appears as a film on the carbon electrode. Based on the XPS and Raman analysis,  $\text{Li}_2\text{CO}_3$  appears to be the discharge product of the  $\text{LiNO}_3$ -type  $\text{Li-CO}_2$  battery.

This study shows that the  $\text{LiNO}_3$ -type battery produces  $\text{Li}_2\text{CO}_3$  as the main product at  $1.7 \text{ e}^-/\text{CO}_2$ , unlike in previous studies.

DEMS analysis was used to measure potential and the amount of  $\text{CO}_2$  that was produced during the  $\text{LiNO}_3$ -type battery charging.

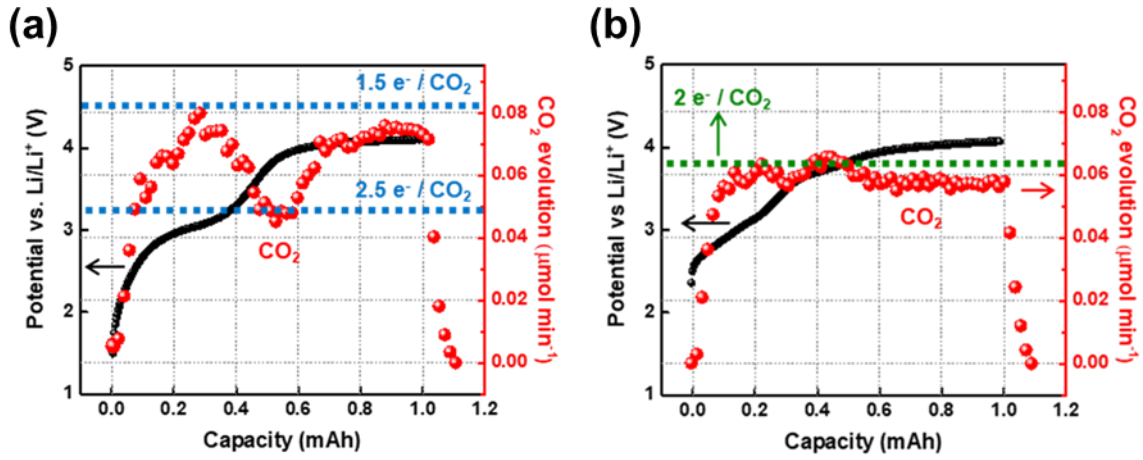


**Figure 1.8** The first charge and CO<sub>2</sub> gas evolution profiles of Li-CO<sub>2</sub> cell, applying a current of 200  $\mu$ A for 5 hours obtained using DEMS analysis in a) the LiTFSI-based electrolyte and b) the LiNO<sub>3</sub>-based electrolyte after 1.0 mAh discharged at pure CO<sub>2</sub> atmosphere.

Fig. 1.8 a) shows the changes in the CO<sub>2</sub> amount and change in potential that occurred when the LiNO<sub>3</sub>-type battery was charged at a current of 200  $\mu$ A. When the Li-CO<sub>2</sub> battery used the conventional electrolyte, most of the potential rapidly increased to more than 4.0 V.<sup>6,36</sup> The generated CO<sub>2</sub> tended to vary according to the potential. In these experiments, the LiNO<sub>3</sub>-type battery charged at around 4.0 V, and the generated CO<sub>2</sub> approached 2.00 e<sup>-</sup>/CO<sub>2</sub> (0.062  $\mu$ mol/min).(figure 1.8b) Based on these results, the LiNO<sub>3</sub>-type Li-CO<sub>2</sub> battery shows lower overpotential and more fixed CO<sub>2</sub> generation than the Li-CO<sub>2</sub> battery.

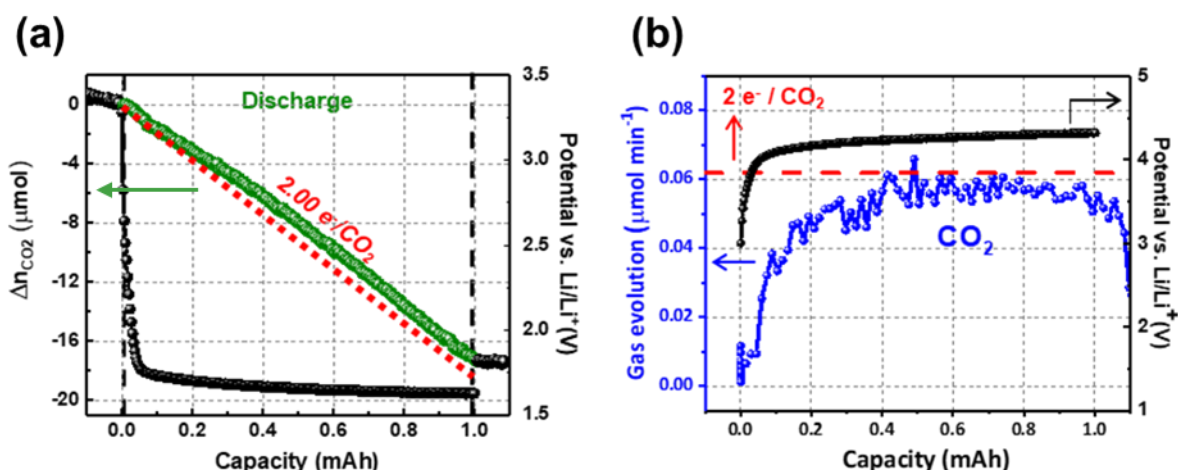


**Figure 1.9** The first discharge a) and charge b) profiles with high concentration 3 M LiNO<sub>3</sub> in DMAc electrolyte. CO<sub>2</sub> gas reduction and oxidation profiles during discharge and charge process of Li-CO<sub>2</sub> cell, applying a current of 200  $\mu\text{A}$  for 5 hours obtained using in-situ DEMS analysis.

Up to now, the mechanism by which CO<sub>2</sub> is fixed and generated before and after charging and discharging has been analyzed. The nitrate-type electrolyte appears to have an intermediate value between a 1.33 and a 2.00-electron process during discharge. During charging, a 2.00-electron process occurs in fig 1.6b and fig 1.8b. We assume that Eq. 1 and the nitrate effect occur simultaneously in the mechanism of CO<sub>2</sub> consumption during discharge.

Therefore, in order to increase the nitrate effect, experiments were performed with a concentration of salt that was higher than that of previous experiments. Fig 1.10 a) shows the CO<sub>2</sub> consumption and potential during discharge. The graph shows that the actual consumed amount was  $\sim 2.10$  e<sup>-</sup>/CO<sub>2</sub>, which is close to a 2.00-electron process. Fig 1.9 b) shows the gas and potential that occurred during charging. The CO<sub>2</sub> occurred at  $0.062 \mu\text{mol min}^{-1}$  (2.00 e<sup>-</sup>/CO<sub>2</sub>) as it did previously. No additional gasses other than CO<sub>2</sub> occurred.

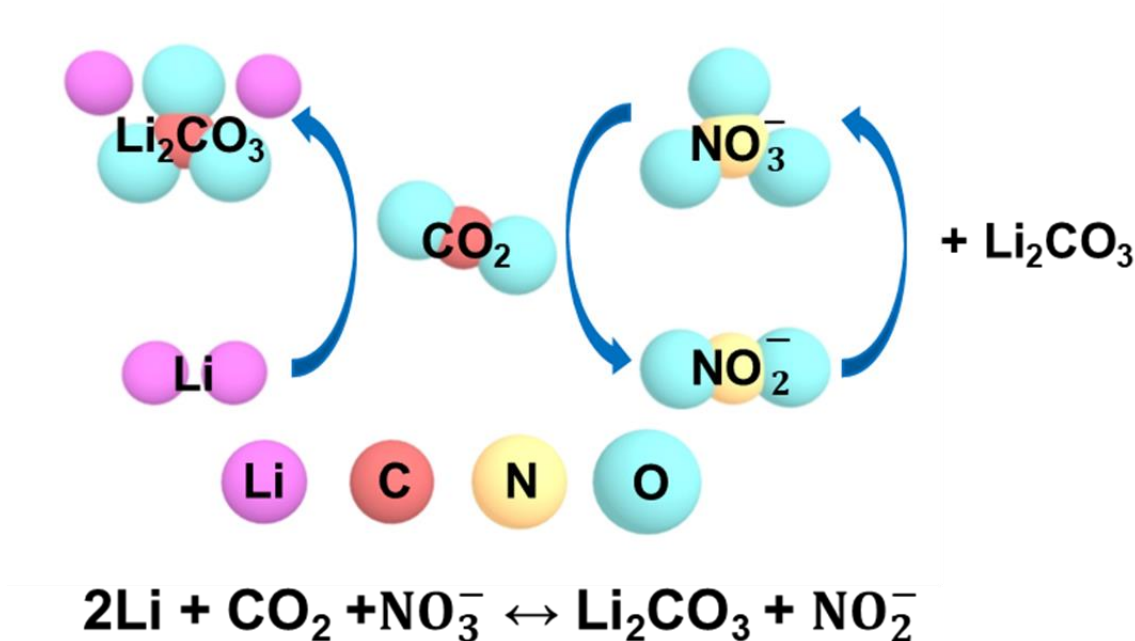


**Figure 1.10** Schematic illustration of the suggestion mechanism in Li- $\text{CO}_2$  using  $\text{LiNO}_3$ -based electrolyte.

Among Li- $\text{CO}_2$  batteries, there have been no reports of  $\text{LiNO}_3$ -based batteries, and the mechanism that was found is not certain. This experiment aims to measure  $\text{CO}_2$  consumption/generation and describe the consumption/generation mechanism. The  $\text{LiNO}_3$ -based Li- $\text{CO}_2$  battery has an  $\sim 1.70 \text{ e}^-/\text{CO}_2$  electron process, which is between  $1.33 \text{ e}^-/\text{CO}_2$  and  $2.00 \text{ e}^-/\text{CO}_2$  during discharge. During charging,  $\text{CO}_2$  generation is fixed at  $2.00 \text{ e}^-/\text{CO}_2$  without generating any additional gasses. High-concentration  $\text{LiNO}_3$ -based batteries show a reversible electron process at  $2.00 \text{ e}^-/\text{CO}_2$  during charging and discharging.

In the Li-air studies reported,  $\text{LiNO}_3$ -based batteries have a 2.00 electron process through the interaction of  $\text{NO}_3^-$  anions. Based on this mechanism, the  $\text{LiNO}_3$ -based Li- $\text{CO}_2$  battery mechanism is shown in Fig. 1.10. In the proposed mechanism, two lithium atoms react with  $\text{CO}_2$  to create the main product  $\text{Li}_2\text{CO}_3$ . The  $\text{NO}_3^-$  anion changes to an  $\text{NO}_2^-$  anion, and the O contributes to the main reaction. Moreover, the  $\text{NO}_2^-$  anion performs the role of a catalyst that decomposes the  $\text{Li}_2\text{CO}_3$  during charging and becomes an  $\text{NO}_3^-$  anion again. According to the proposed mechanism, the  $\text{LiNO}_3$ -based Li- $\text{CO}_2$  battery has a reversible reaction, and it creates a charging reaction at a lower overpotential through the redox-shuttle effect of the nitrate anion.

## 1.6 Conclusion

It is difficult to obtain a reversible reaction involving  $\text{CO}_2$  in  $\text{Li-CO}_2$  batteries during electrochemical reactions. In this study, a reversible reaction was obtained using a nitrate-based electrolyte.  $\text{CO}_2$  consumption and evolution exhibited a two-electron process during both the charge and the discharge.

It was also confirmed that the process is maintained at high-concentration conditions. Moreover, XPS and Raman analysis confirmed that only  $\text{Li}_2\text{CO}_3$  was produced without additional products. Thus far, there have been no reports of nitrate-based electrolytes in research regarding  $\text{Li-CO}_2$  batteries to the best of our knowledge. There is also insufficient research on the interactions of electrolytes with  $\text{CO}_2$ . This study presents the possibility of applying a new mechanism and a new electrolyte in  $\text{Li-CO}_2$  batteries, based on which various electrolytes can be developed with reference to  $\text{Li-O}_2$  battery, as it is necessary to develop  $\text{Li-CO}_2$  batteries exhibiting reversible reactions and low overpotential.

## 1.7 Experimental section

**Li-CO<sub>2</sub> Cell Assembly.** For the preparation of the cathode for the aprotic electrolyte, the air cathode was fabricated using a mixture of Ketjenblack carbon (EC-300J) and polytetrafluoroethylene (PTFE, Sigma-Aldrich, USA) at 9:1 (wt%). The mixture was dispersed in water solution and cast on an SUS mesh (stainless steel mesh, Shinmyung Science Inc.) current collector, and then was dried at 120 °C in a vacuum oven overnight. The cathode loading mass was approximately 0.3 mg/cm<sup>2</sup>.

1 M LiTFSI (Lithium bis(trifluoromethanesulfonyl)imide) in the TEGDME (Tetraethylene glycol dimethyl ether) and 1 M LiNO<sub>3</sub> in the DMAc (dimethylacetamide) were purchased from Enchem (Korea) and stored in an Ar-filled glove box (H<sub>2</sub>O and O<sub>2</sub> < 1 ppm).

3 M LiNO<sub>3</sub> in the DMAc were fabricated using LiNO<sub>3</sub> salt (Sigma Aldrich, ReagentPlus) and DMAc solvent (Sigma Aldrich, anhydrous 99.8%). The Li-CO<sub>2</sub> cell was assembled into a 2032 coin cell (Hohsen, CR2032, Japan) with holes. The Li metal film (thickness of 0.3 mm) was purchased from FMC (Korea). The glass fiber separator (GF/C) was purchased from Whatman (England). The Li-CO<sub>2</sub> cell assembly was carried out in an Ar-filled glove box.

**Material Characterizations** The carbon cathode were analyzed by using a SEM (S-4800, Hitachi High Technologies, Japan) at an acceleration voltage of 5.0 kV and XPS experiments were performed on a scanning X-ray microprobe (ESCALAB 250XI, Thermo Fisher scientific, US). Raman spectra were measured by a micro Raman spectroscope (alpha 300, WITec GmbH) using 532 nm. Before the cathodes were transferred to SEM and XPS analysis after cell disassembly, they were packed in an Ar-filled glove box to prevent contamination of products on electrode from the air.

**Electrochemical Measurements.** Galvanostatic discharge-charge was used to evaluate battery performance (capacity, voltage, power density) by using a battery cycler system (WBCS 3000, WonATech, Korea). For the experiments performed, the Li-CO<sub>2</sub> cells using aprotic electrolytes were tested at room temperature in a lab-built coin cell kit. The details of the differential electrochemical mass spectrometer (DEMS) system are described elsewhere.<sup>33</sup>

## References

1. Matter, J. M.; Stute, M.; Snæbjörnsdóttir, S. O.; Oelkers, E. H.; Gislason, S. R.; Aradóttir, E. S.; Sigfusson, B.; Gunnarsson, I.; Sigurdardóttir, H.; Gunnlaugsson, E.; Axelsson, G.; Alfredsson, H. A.; Wolff-Boenisch, D.; Mesfin, K.; Taya, D. F. d. l. R.; Hall, J.; Dideriksen, K.; Broecker, W. S., Rapid carbon mineralization for permanent disposal of anthropogenic carbon dioxide emissions. *Science* **2016**, 352, 1312-1314
2. Rochelle, G. T., Amine scrubbing for CO<sub>2</sub> capture. *Science* **2009**, 325, 1652-1654
3. Graciani, J.; Mudiyanse, K.; Xu, F.; Baber, A. E.; Evans, J.; Senanayake, S. D.; Stacchiolar, D. J.; Liu, P.; Hrbek, J.; Sanz, J. F.; Rodriguez, J. A., Catalysis. Highly active copper-ceria and copper-ceria-titania catalysts for methanol synthesis from CO<sub>2</sub>. *Science* **2014**, 345, 546-550
4. Ren, D.; Deng, Y.; Handoko, A. D.; Chen, C. S.; Malkhandi, S.; Yeo, B. S., Selective electrochemical reduction of carbon dioxide to ethylene and ethanol on copper(I) oxide catalysts. *ACS Catal* **2015**, 5, 2814-2821
5. Costentin, C.; Drouet, S.; Robert, M.; Savéant, J.-M., A local proton source enhances CO<sub>2</sub> electroreduction to CO by a molecular Fe catalyst. *Science* **2012**, 338, 90-94
6. Qiao, Y.; Yi, J.; Wu, S.; Liu, Y.; Yang, S.; He, P.; Zhou, H., Li-CO<sub>2</sub> Electrochemistry: A New Strategy for CO<sub>2</sub> Fixation and Energy Storage. *Joule* **2017**, volume 1, Issue 2, 11, 359-370
7. Xu, S.; Das, S. K.; Archer, L. A., The Li-CO<sub>2</sub> battery: a novel method for CO<sub>2</sub> capture and utilization. *RSC advances* **2013**, 3 (18), 6656-6660
8. Takechi, K.; Shiga, T.; Asaoka, T., A Li-O<sub>2</sub>/CO<sub>2</sub> battery. *Chemical communications* **2011**, 47 (12), 3463-3465
9. Li, J.; Zhao, H.; Qi, H.; Sun, X.; Song, X.; Guo, Z.; Tamirat, A. G.; Liu, J.; Wang, L.; Feng, S., Drawing a Pencil-Trace Cathode for a High-Performance Polymer-Based Li-CO<sub>2</sub> Battery with Redox Mediator. *Adv. Funct. Mater.* **2019**, 29, 1806863
10. Yang, S.; He, P.; Zhou, H., Exploring the electrochemical reaction mechanism of carbonate oxidation in Li-air/CO<sub>2</sub> battery through tracing missing oxygen. *Energy Environ. Sci* **2016**, 9, 1650
11. Wang, Y.; Cho, S. C., Analysis of Air Cathode Performance for Lithium-Air Batteries. *Journal of The Electrochemical Society* **2013**, 160 (10) A1847-A1855
12. Qie, L.; Connell, J. W.; Xu, J.; Dai, L., Highly rechargeable Li-CO<sub>2</sub> batteries with a boron and nitrogen-codoped holey graphene cathode. *Angew. Chem. Int. Ed* **2017**, 56, 6970-6974
13. Zhang, X.; Zhang, Q.; Zhang, Z.; Chen, Y.; Xie, Z.; Wei, J.; Zhou, Z., Rechargeable Li-CO<sub>2</sub> batteries with carbon nanotubes as air cathode. *Chem. Commun* **2015**, 51, 14636-14639
14. Li, Y.; Zhou, J.; Zhang, T.; Wang, T.; Li, X.; Jia, Y.; Cheng, J.; Guan, Q.; Liu, E.; Peng, H.; Wang, B., Highly surface wrinkled and N-doped CNTs anchored on metal wire. *Adv. Funct. Mater* **2019**, 29, 1808117



15. Zhang, Z.; Zhang, Z.; Liu, P.; Wie, Y.; Cao, K.; Zhou, Z., Identification of cathode stability in Li–CO<sub>2</sub> batteries with Cu nanoparticles highly dispersed on N-doped graphene. *J. Mater. Chem. A* **2018**, 6, 3218-3223
16. Pipes, R.; Bhargav, A.; Manthiram, A., Nanostructured Anatase Titania as a Cathode Catalyst for Li–CO<sub>2</sub> Batteries. *ACS Appl. Mater. Interfaces* **2018**, 10, 43, 37119-37124
17. Zhang, X.; Wang, C.; Li, H.; Wang, W. -G.; Chen, Y. -N.; Xie, Z.; Zhou, Z., High performance Li–CO<sub>2</sub> batteries with NiO–CNT cathodes. *J. Mater. Chem. A* **2018**, 6, 2792-2796
18. Hou, Y.; Wang, J.; Liu, L.; Liu, Y.; Chou, S.; Shi, D.; Liu, H.; Wu, T.; Zhang, W.; Chen, J., Mo<sub>2</sub>C/CNT: An Efficient Catalyst for Rechargeable Li–CO<sub>2</sub> Batteries. *Adv. Funct. Mater* **2017**, 27, 1700564
19. Yang, S.; Qiao, Y.; Liu, Y.; Cheng, Z.; Zhu, J. -J.; Zhou, H., A reversible lithium–CO<sub>2</sub> battery with Ru nanoparticles as a cathode catalyst. *Energy Environ. Sci* **2017**, 10, 972-978
20. Bie, S.; Du, M.; He, W.; Zhang, H.; Yu, Z.; Liu, J.; Liu, M.; Yan, W.; Zhou, L.; Zhou, Z., Carbon Nanotube@RuO<sub>2</sub> as a High Performance Catalyst for Li–CO<sub>2</sub> Batteries. *ACS Appl. Mater. Interfaces* **2019**, 11, 5, 5146-5151
21. Liang, H.; Zhang, Y.; Chen, F.; Jing, S.; Yin, S.; Tsiakaras, P., A novel NiFe@NC-functionalized N-doped carbon microtubule network derived from biomass as a highly efficient 3D free-standing cathode for Li-CO<sub>2</sub> batteries. *Applied Catalysis B: Environmental* **2019**, 244, 559-567
22. Park, J. -B.; Lee, S. H.; Jung, H. -G.; Aurbach, D.; Sun, Y. -K., Redox Mediators for Li–O<sub>2</sub> Batteries: Status and Perspectives. *Adv. Mater* **2018**, 30, 1704162
23. Kwak, W. -J.; Kim, H.; Jung, H. -G.; Aurbach, D.; Sun, Y. -K., Review—A Comparative Evaluation of Redox Mediators for Li-O<sub>2</sub> Batteries: A Critical Review. *Journal of The Electrochemical Society* **2018**, 165 (10) A2274-A2293
24. Wang, X. -G.; Wang, C.; Xie, Z.; Zhang, X.; Chen, Y.; Wu, D.; Zhou, Z., Improving Electrochemical Performances of Rechargeable Li-CO<sub>2</sub> Batteries with an Electrolyte Redox Mediator. *ChemElectroChem* **2017**, 4, 2145–2149
25. Li, J.; Zhao, H.; Qi, H.; Sun, X.; Song, X.; Guo, Z.; Tamirat, A. G.; Liu, J.; Wang, L.; Feng, S., Drawing a Pencil- Trace Cathode for a High- Performance Polymer- Based Li–CO<sub>2</sub> Battery with Redox Mediator. *Adv. Funct. Mater* **2019**, 29, 1806863
26. Lee, S. H.; Park, J. -B.; Lim, H. -S.; Sun, Y. -K., An Advanced Separator for Li–O<sub>2</sub> Batteries: Maximizing the Effect of Redox Mediators. *Adv. Energy Mater* **2017**, 7, 1602417
27. Uddin, J.; Bryantsev, V. S.; Giordani, V.; Walker, W.; Chase, G. V.; Addison, D., Lithium Nitrate As Regenerable SEI Stabilizing Agent for Rechargeable Li/O<sub>2</sub> Batteries. *J. Phys. Chem. Lett* **2013**, 4, 21, 3760-3765
28. Xia, C.; Kwok, C. Y.; Nazar, L. F., A high-energy-density lithium-oxygen battery based on a reversible four-electron conversion to lithium oxide. *Science* **2018**, 361, 777–781

29. Yoo, E.; Qiao, Y.; Zhou, H., Understanding the effect of the concentration of LiNO<sub>3</sub> salt in Li–O<sub>2</sub> batteries. *J. Mater. Chem. A* **2019**, 7, 18318–18323
30. Giordani, V.; Tozier, D.; Uddin, J.; Tan, H.; Gallant, B. M.; McCloskey, B. D.; Greer, J. R.; Chase, G. V.; Addison, D., Rechargeable-battery chemistry based on lithium oxide growth through nitrate anion redox. *Nature Chemistry* **2019**, volume 11, 1133–1138
31. Reproduced in part with permission from Baek, K. E.; Lee, J. G.; Cha, A. M.; Lee, J. S.; An, K. J.; Kang, S. J., Chemically impregnated NiO catalyst for molten electrolyte based gas-tank-free LiO<sub>2</sub> battery. *Journal of Power Sources* **2018**, 402, 68
32. Walker, W.; Giordani, V.; Uddin, J.; Bryantsev, V. S.; Chase, G. V.; Addison, D., A Rechargeable Li–O<sub>2</sub> Battery Using a Lithium Nitrate/N,N-Dimethylacetamide Electrolyte. *J. Am. Chem. Soc* **2013**, 135, 6, 2076-2079
33. McCloskey, B. D.; Bethune, D. S.; Girishkumar, G.; Luntz, A. C., Solvents' Critical Role in Nonaqueous Lithium–Oxygen Battery Electrochemistry. *J. Phys. Chem. Lett* **2011**, 2, 10, 1161-1166
34. Wood, K. N.; Teeter, G., XPS on Li-Battery-Related Compounds: Analysis of Inorganic SEI Phases and a Methodology for Charge Correction. *ACS Appl. Energy Mater* **2018**, 1, 9, 4493-4504
35. Pasierb, P.; Komornicki, S.; Rokita, M.; Rekas, M., Structural properties of Li<sub>2</sub>CO<sub>3</sub>–BaCO<sub>3</sub> system derived from IR and Raman spectroscopy. *Journal of Molecular Structure* **2011**, Volume 596, Issues 1–3, 26, 151-156
36. Zhang, Z.; Wang, X. G.; Zhang, X.; Xie, Z.; Chen, Y. N.; Ma, L.; Peng, Z.; Zhou, Z., Verifying the Rechargeability of Li-CO<sub>2</sub> Batteries on Working Cathodes of Ni Nanoparticles Highly Dispersed on N-Doped Graphene. *Adv. Sci* **2018**, 5, 1700567

